Available online at www.sciencedirect.com
SCIENCE DIRECT
International Journal of Pharmaceutics 310 (2006) 15–24
INTERNATIONAL JOURNAL OF PHARMACEUTICS
www.elsevier.com/locate/ijpharm

An in vitro study of the design and development of a novel doughnut-shaped minitablet for intraocular implantation

Yahya E. Choonara [a], Viness Pillay [a], Trevor Carmichael [b], Michael P. Danckwerts [a,*]

[a] *University of the Witwatersrand, Department of Pharmacy and Pharmacology, 7 York Road, Parktown 2193, Johannesburg, Gauteng, South Africa*
[b] *Department of Ophthalmology, Faculty of Health Sciences, 7 York Road, Parktown 2193, Johannesburg, Gauteng, South Africa*

Received 26 August 2005; received in revised form 13 October 2005; accepted 15 October 2005
Available online 7 February 2006

Abstract

A novel doughnut-shaped minitablet (DSMT) was developed and evaluated as a biodegradable intraocular drug delivery system for rate-modulated delivery of antiviral bioactives. The DSMT device was manufactured using a special set of punches fitted with a central-rod in a Manesty tableting press. The DSMT device released the antiretrovirals foscarnet and ganciclovir at a first-order rate. The erosion kinetics was assessed by gravimetric analysis and scanning electron microscopy. The device gradually eroded when immersed in simulated vitreous humor (SVH) (pH 7.4, 37 °C) and released bioactives in a sustained manner. The novel geometric design and veracity of the DSMT device was retained even after 24 weeks of erosion. When considering the duration of the bioactive released from the DSMT device, it was found that by the careful selection of the type and concentration of polymer employed in formulating the DSMT device, it was possible to produce a device that could release drug for any period up to 12 months.

Keywords: Cytomegalovirus retinitis; Doughnut-shaped minitablet (DSMT); Extended release; Polylactide-*co*-glycolide (PLGA); Biodegradation; Intraocular implantation

1. Introduction

Disease due to cytomegalovirus (CMV) is among the most common opportunistic infections in patients with the acquired immune deficiency syndrome (AIDS). The virus can give rise to multiple organ disease and may cause infections such as colitis, esophagitis, encephalitis and pneumonitis, but retinitis accounts for 75–85% of CMV infections in patients (Jabs et al., 2003). CMV retinitis (CMV-R) causes severe visual loss and needs medical treatment for an optimal clinical outcome. It is a serious sight-threatening infection that occurs in approximately 25% of patients with AIDS. If left untreated the disease follows a relentless course which inevitably results in blindness (Smith et al., 1992).

Prospective epidemiological studies have estimated the risk of CMV-R in patients with CD4+ counts less than 100 cells/mm^3 at approximately 10% per year, and in those with CD4+ counts less than 50 cells/mm^3 at approximately 20% per year. Patients with CD4+ counts above 200 cells/mm^3 have rarely developed CMV-R. However, this could change in the future with widespread use of highly active antiretroviral therapy that dramatically changes absolute CD4+ counts (Lin et al., 2002; Holbrook et al., 2003).

Both eyes can be infected at different times with more than one focus of retinitis. Retina that is destroyed by the virus is irreversibly lost and blindness occurs as soon as areas that are critical for vision, including the macula, maculopapillary nerve fibre layer bundle and optic nerve head, become infected (Holland et al., 1987, 1989). In the early stages of CMV-R, patients may notice changes in vision, floating particles or loss of peripheral vision. The disease is not associated with light sensitivity, pain, or redness of the eye. Patients with AIDS should be screened regularly as early diagnosis and efficient management are essential to preserve visual function, and preservation of visual function is a major objective to assure good quality of life (Yasukawa et al., 2000).

Treatment of CMV-R requires chronic suppressive maintenance therapy with an anti-cytomegaloviral drug to prevent or

* Corresponding author. Tel.: +27 11 7172052; fax: +27 11 6424355.
E-mail address: danckwertsmp@therapy.wits.ac.za (M.P. Danckwerts).

0378-5173/$ – see front matter © 2005 Elsevier B.V. All rights reserved.
doi:10.1016/j.ijpharm.2005.10.019

delay relapse of the disease (Jabs et al., 2003). With each relapse, additional retinal destruction takes place, causing further loss of visual function. Delivery of antiviral drugs to the vitreous cavity has been attempted by various routes, which suffer from some weakness or the other (Kumar et al., 2001). There are currently three different types of dosage forms available for intravitreal CMV-R therapy. These are: the intravitreal injections of ganciclovir, foscarnet, cidofovir, or formivirsen (Diaz-Llopis et al., 1994; Rosanne, 2001), microspheres/nanoparticles of ganciclovir (Herroro-Vanrell and Ramirez, 2000; Merodio et al., 2001), and the ganciclovir implant (Vitrasert®) which was licensed in March 1996 (Sanborn et al., 1992).

The Vitrasert® implant (Chiron Vision Inc., Irvine, California) which was developed and approved by the US Food and Drug Administration (FDA) has been used with some success in practice for the treatment of CMV-R (Hatton et al., 1998; Davis et al., 1999; Perkins et al., 2001). It is a sustained-release intraocular implant consisting of semi-permeable polymers containing a 6 mg ganciclovir pellet.

The intravitreal route of administration is more preferable to the IV route when treating patients with CMV-R (Cochereau-Massin et al., 1991). Intravitreal ganciclovir and foscarnet injections provide higher intraocular drug concentrations than systemic exposure to drug. Although the intravitreal route is suitable for the treatment of CMV-R, it still remains a highly invasive and difficult route for administration. Among the most promising developments are intraocular implants/devices designed to deliver drugs with precision directly to the vitreous humor, retina, and choroid (Ashton et al., 1992). Local delivery of drugs to the eye via intravitreal implants offers several advantages over systemic and intravitreal injection therapy.

Firstly, it bypasses the blood–ocular barriers, allowing higher intraocular drug levels than could normally be achieved by systemic administration. Secondly, it avoids many of the side effects associated with systemic and intravitreal injection therapy and provides relatively constant drug levels in the eye. Finally, much less drug is needed for this local drug delivery, which is especially important for newer therapeutic agents that may be in short supply or are extremely expensive (Musch et al., 1997).

The polymers employed in manufacturing the Vitrasert® device are not biodegradable and this requires the implant to be removed from the vitreous humour once its drug load has been depleted. It is also extremely complicated to manufacture, as it requires a number of carefully controlled coating processes. The complication of separation of the ganciclovir pellet from the flange (suture tab) during the removal of the Vitrasert® implant has also been observed. Furthermore, removal of the implant may produce vitreous traction that could potentially increase the risk of retinal detachment and poor wound healing from multiple surgical procedures. This may increase the risk of a wound leaking (Martin et al., 1997). Lastly, the cost of such a device is approximately US$ 5000, which is not an option for the average CMV-R patient with HIV/AIDS.

Therefore, the objective of this study was to develop a small implantable doughnut-shaped minitablet (DSMT) and explore the physicochemical characteristics of this novel drug delivery system using poly(lactic-*co*-glycolic) acid polymer combinations in order to solve the problem of the implant not being biodegradable. The small DSMT can be neatly sutured to the scleral flap with a biodegradable suture where it could release bioactive antivirals over a number of months. Since it will be a bioerodible system, there will be no need to remove the device once it has released its entire drug load. The device will be easy to manufacture, and is reproducible as it is produced on a tableting press.

It is critical that the DSMT device remains intact during its period of implantation, as well as retain the ability to be easily manufactured using a conventional tableting press, therefore this work also focused on pharmaceutical preformulation studies. The micromeritic properties, flowability and compressibility of the materials were investigated and evaluated for their suitability in fabricating the DSMT device. The degradation mechanism of the DSMT device which will ultimately lead to complete erosion of the device when implanted in the posterior segment of the eye was also explored.

A schematic illustration of the envisaged implantation of the DSMT device in the human eye is depicted in Fig. 1. To ascertain the ability of the DSMT device to release antiviral bioactives from its matrix structure in vitro release studies were performed in 4 ml of simulated vitreous humor (SVH) (i.e. phosphate buffered saline (PBS) containing 0.03% hyaluronic acid, pH 7.4, 37 °C) utilizing a modified USP XXV dissolution testing apparatus.

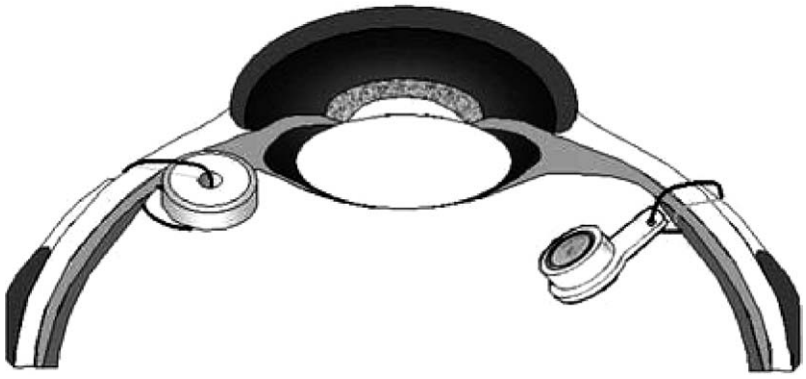

Fig. 1. Envisaged implantation of the DSMT device in the human eye with a Vitrasert® device for comparison.

2. Materials and methods

Resomer® grades RG502, RG503, RG504, and RG756 consisting of poly(lactide-*co*-glycolide) (PLGA) with a 50% lactide content, were purchased from Boehringer Ingelheim (Ingelheim, Germany). These polymers are all biodegradable and have inherent viscosities ranging from 0.16 to 8.2 dl/g. All polymers were ground in a mortar and the fraction passing through a sieve with an aperture size of 125 μm (Endcotts Test Sieves Ltd., London, United Kingdom) was used. Phosphonoformic acid (Foscarnet) was obtained from Sigma–Aldrich Co. (Aldrich, Germany). Ganciclovir was purchased from Roche Products (Pty) Ltd. (Isando, South Africa). The antiviral bioactives were also passed through a sieve with an aperture size of 125 μm prior to use.

2.1. Preparation of the DSMT device

A specially designed punch set was provided by P.A. Cuthbert & Co. (Pty) Ltd. (London, United Kingdom) and engineered by Holland Tableting Science (London, United Kingdom). The punch set consisted of a lower and upper punch, die, and central-rod, as shown in the schematic (Fig. 2). Both the upper and lower punches contained a longitudinal central hole for the insertion of the rod, which enabled a doughnut-shaped tablet to be compressed around it. The specifications of the punch set are listed in Table 1.

All blending of drug and polymer was performed using an Erweka AR 400 Cube Blender at 50 rpm (Erweka, Germany), and a Manesty F3 eccentric (single punch) tableting press (Manesty Machines, United Kingdom) was used for directly compressing the powder blends into the DSMT device. A model TR 104 mass balance supplied by the Denver Instrument Company (Denver, USA) was used for all gravimetrical analysis.

The directly compressed formulations consisted of two principal components, namely, the antiviral bioactives and the various biodegradable polymers. With the appropriate choice of polymer, compression of the mixture led to the formation of a matrix tablet. To study the influence of different variables on the release rate of the DSMT device, formulations containing various concentrations of bioactive material were produced, and at the same time, the polymer grades were varied to produce different implants.

DSMT devices were produced consisting of 30, 40, 50, 60, and 70% (w/w) foscarnet and 10, 15, and 20% (w/w) ganciclovir, in each of the three Resomer® grades chosen in fabricating the device. These concentrations were selected on the basis of the dose required for each bioactive in treating CMV-R over a sustained period of time.

Table 1
Specifications of the novel tooling used to compress the DSMT device

Tooling	Diameter (mm)	Inner hole (mm)	Length (mm)
Upper punch	5.00	2.00	47.00
Lower punch	5.00	2.00	52.00
Central rod	2.00	N/A	305.00
Die	40.00	6.00	20.00

The various formulations were individually pre-weighed and blended for 10 min and then manually fed into the die cavity. The press was set to compress DSMT devices to a thickness of 2 mm. The variation in compression forces were accomplished by firstly adjusting the upper punch to its lowest position in order to ensure a maximum stable compression force exerted from above, while adjusting the lower punch accordingly by elevating the punch for higher compression forces, or alternatively lowering it for lower compression forces. The adjustments on the lower punch were executed using inherent calibration marks positioned on the adjustment bearing of the tableting press. The flywheel of the tablet press was then twisted backward as far as possible (to the limit where the lower punch started to rise again).

This was done to ensure that the tablet press would have enough time to speed up to a relatively constant velocity during compression. The powder blends were then compressed at room temperature. Fig. 3 illustrates a schematic diagram of the production sequence.

2.2. Textural analysis

Textural analysis was employed to characterize the compressibility of the polymers used in fabricating the DSMT device, employing the *TA.XTplus* Texture Analyzer (Stable Micro Systems, England) fitted with a probe having a spherical indenter of 3.125 mm in diameter and a 5 kg load cell. The indentation hardness was represented by a conversion to the Brinell Hardness Number (BHN) (Eq. (1)). The textural settings used to calculate the BHN values are depicted in Table 2.

Table 2
Textural settings employed for BHN value calculations

Test Parameters	Settings
Pre-test speed (mm/s)	1.000
Test speed (mm/s)	0.500
Post-test speed (mm/s)	1.000
Compressive distance (mm)	0.250
Trigger force (N)	0.050

Fig. 4 illustrates typical force–displacement profiles generated for the calculation of the BHN value.

$$\mathrm{BHN} = \frac{2F}{\pi D(D^2 - d^2)^{1/2}} \quad (1)$$

where F is the force generated from indentation, D the diameter of spherical probe indenter (3.175 mm), and d the indentation depth (0.25 mm).

2.3. Erosion studies

Mass loss of the DSMT matrix was evaluated by gravimetrical analysis. Individual DSMT devices were initially weighed,

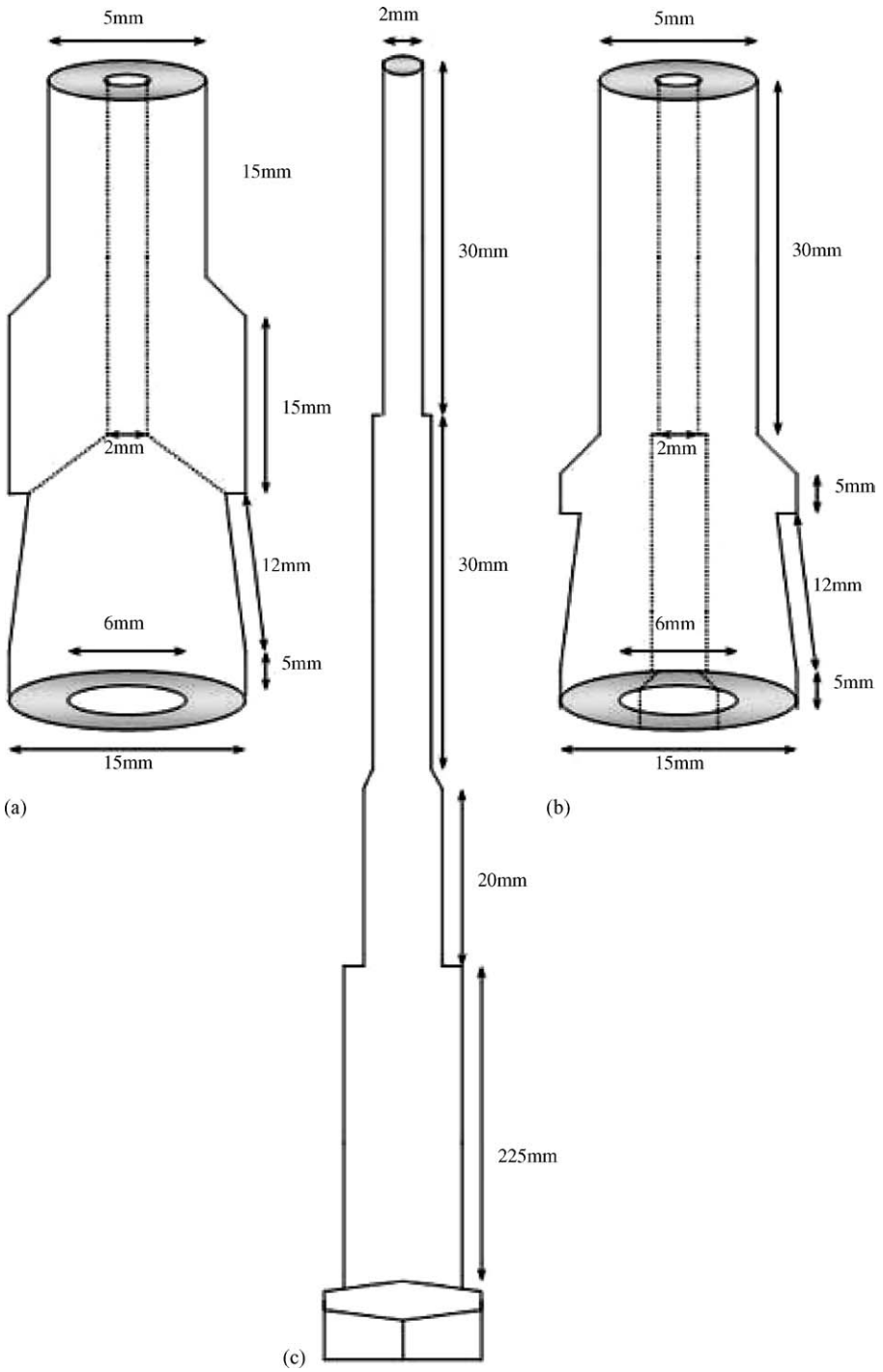

Fig. 2. The novel DSMT tooling: (a) lower punch; (b) upper punch; and (c) central-rod.

after which degradation was allowed to progress in 4 ml of SVH (pH 7.4, 37 °C) in an oscillating laboratory incubator (Labcon® FSIE-SPO 8–35, California, USA) set to oscillate at 50 rpm. At predetermined intervals the DSMTs were removed from the vials incubated and gently rinsed with deionised water to remove any superficial particles resulting from undissolved buffer salts. The hydrated matrices were then vacuum-dried and weighed accordingly to assess any gravimetric changes. All experiments were performed in triplicate. The initial and final masses were used to calculate the percentage mass loss (ML%) using Eq. (2):

$$\mathrm{ML\%} = 100\frac{(W_o - W_r)}{W_o} \tag{2}$$

where W_0 is the initial mass of the device and W_r the residual mass of the same dried and partially eroded device.

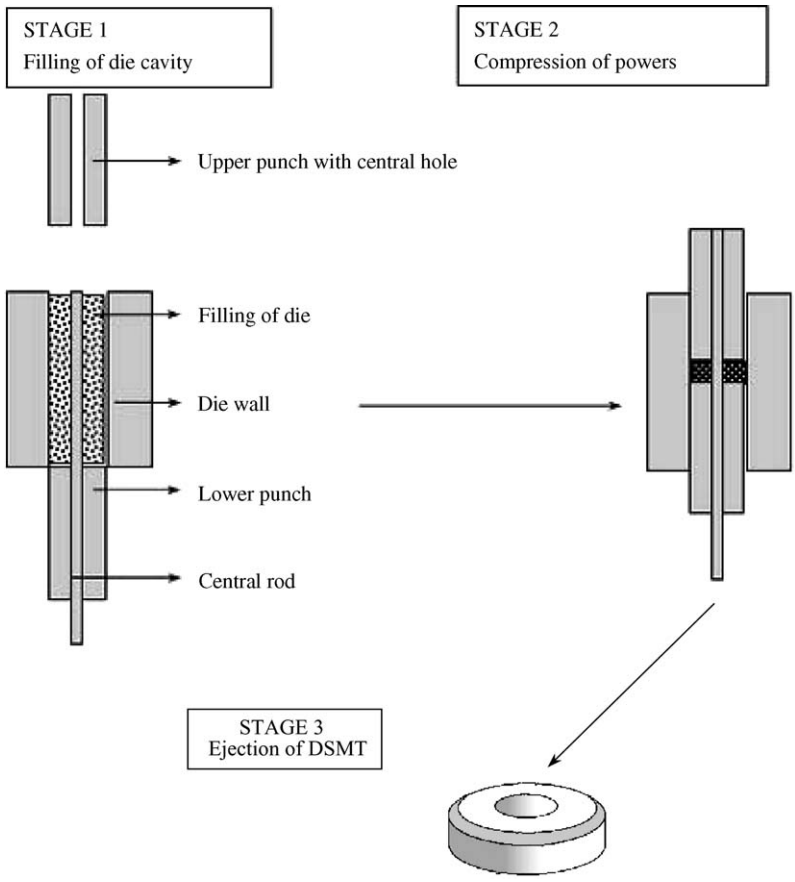

Fig. 3. Schematic of a production sequence for the doughnut-shaped minitablet (DSMT) device.

2.4. Scanning electron microscopy

Samples were prepared for photomicrographs by applying a thin layer of colloidal graphite on aluminum stubs and mounting the DSMT devices on the graphite to hold them in place during microscopic examination. The devices were then coated with a thin layer of gold–platinum using a sputter coater under an electrical potential of 15 kV. Several photomicrographs were produced by scanning fields, selected at different magnifications using a Jeol JSM-840 scanning electron microscope (Tokyo, Japan).

2.5. In vitro drug release studies

A modified closed-compartment USP XXV dissolution testing apparatus was utilized in performing all the release studies. At time zero, the DSMT devices were immersed in 4 ml of simulated vitreous humor (SVH) (i.e. PBS with 0.03% hyaluronic

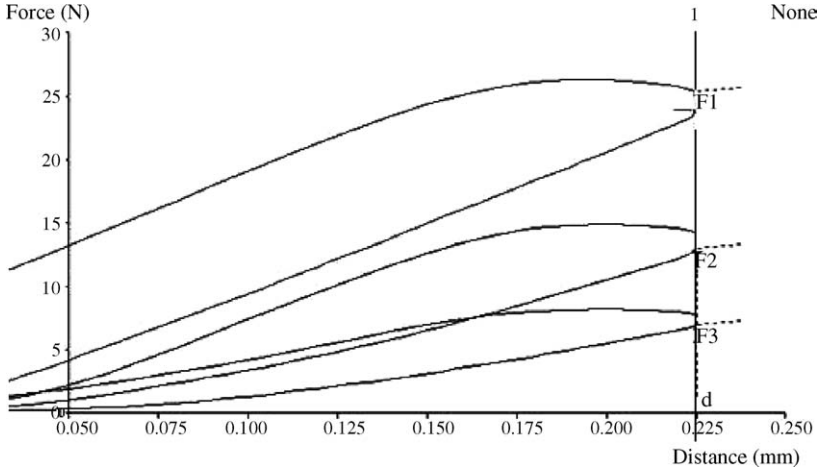

Fig. 4. Typical force–displacement profiles for PLGA compacts used in the determination of matrix indentation hardness.

acid, pH 7.4, 37 °C) in closed vials and placed in an oscillating laboratory incubator (Labcon® FSIE-SPO 8–35, California, USA) set to at 50 rpm. At predetermined intervals, 2 ml of the release medium was sampled and 2 ml of fresh SVH was replaced to the sampled vial to maintain sink conditions.

2.6. Analysis of the antiviral bioactives

Analyses of foscarnet and ganciclovir were performed on a System Gold (Beckman, San Ramon, California) high-performance liquid chromatograph (HPLC) equipped with a 20 μl loop, and array detector. The system was fitted with a Discovery C_{18} (particle size 5 μm, 4.6 mm i.d., 150 mm) analytical column (Supelco, USA). Samples of 20 μl were injected using a microlitre syringe (705 NR 50 μl, Hamilton Bonaduz AG, Switzerland). The HPLC method was validated by undertaking a precision and accuracy analysis of sample replicates both inter- and intra-day. The coefficient of variation for both precision and accuracy studies was within suitable limits namely 1.25 and 1.79%, respectively.

The mobile phase for analysing foscarnet samples was composed of 0.005 M sulphuric acid/methanol (95:5%, v/v) and approximately 0.09% (w/v) of tetrahexylammonium hydrogensulphate ($THAHSO_4$) as an ion-pairing reagent. A solvent flow rate of 1.5 ml/min was maintained. In the case of ganciclovir, the mobile phase was composed of 0.05 M ammonium acetate (pH 6.5)/acetonitrile (96:4%, v/v), and a solvent flow rate of 1.0 ml/min was maintained. Prior to use, the column was equilibrated by passing 45 ml of solvent through the system. The eluant was monitored at an analytical wavelength set at 254 nm. The entire assay procedure was performed at room temperature. Ascorbic acid and acyclovir were used as the respective internal standards for foscarnet and ganciclovir analysis.

3. Results and discussion

3.1. Compressibility of the PLGA polymers employing textural analysis

Table 3 lists the force values (*N*) generated from indentation of the PLGA compacts, as well as the BHN values. The compressibility profiles for each polymer investigated are shown in Fig. 5(a–d). The indentation hardness of the compacts indicated that the material formed moderately soft compacts, as the compression force increased. Notably, the BHN values for the amorphous regions of the polymer in the DSMT showed significant variability as seen from the compressibility profiles obtained in Fig. 5(a–d). This behaviour was contrary to that expected. One observation was that the sudden upward trend (Fig. 5(b and d)) of the compressibility profile at a compression force of 7.50 t could possibly be attributed to an increase in crystallinity of the PLGA compacts as a result of amorphous regions being subjected to deformation earlier than the crystalline regions during application of compression force. Hence, this leads to an increase in crystallinity in the remaining polymer and thus a higher BHN value.

Table 3
BHN values obtained at the different compression forces

Polymer type	Compression force (t)	Indentation force (N)[a], mean ± S.D.	BHN (N/mm^2)[a], mean ± S.D.
Resomer® RG502	2.50	26.228 ± 0.216	150.338 ± 1.240
Resomer® RG502	5.00	25.955 ± 0.302	148.773 ± 1.731
Resomer® RG502	7.50	26.382 ± 0.375	151.221 ± 2.148
Resomer® RG503	2.50	25.852 ± 0.349	148.183 ± 2.006
Resomer® RG503	5.00	26.355 ± 0.120	151.066 ± 0.689
Resomer® RG503	7.50	26.525 ± 0.912	152.041 ± 0.523
Resomer® RG504	2.50	26.396 ± 1.062	151.301 ± 6.089
Resomer® RG504	5.00	24.426 ± 1.184	140.009 ± 6.785
Resomer® RG504	7.50	26.100 ± 0.368	149.605 ± 2.107
Resomer® L214	2.50	26.152 ± 0.816	149.903 ± 4.678
Resomer® L214	5.00	24.934 ± 0.235	142.921 ± 1.346
Resomer® L214	7.50	24.602 ± 0.411	141.018 ± 2.356

[a] Force produced on indentation of compacts.

This observation highlights the important differences in the mechanical properties of amorphous pharmaceutical material, which is temperature and pressure dependant in their response to applied mechanical stress. Firstly, the copolymer PLGA is an amorphous type material. Amorphous materials do not have melting points but rather go through a glass transition temperature (T_g). PLGA 50:50 has a T_g value of 39.85 °C. Secondly, poly(lactide) (PLA) is thermally unstable (Zhang et al., 1992).

Hence, the presence of this monomer randomly distributed within the copolymer backbone structure tends to increase chain flexibility and therefore, at elevated temperatures during the direct compression technique, it is inclined to contribute to the opening of the polymer structure and widening in the copolymer molecular weight distribution and a decrease in yield pressure. The yield pressure indicates the point where forces involved in consolidation have essentially been 'broken'. The yield pressure for PLGA is well below the lowest pressure used in the compressibility of the DSMT's and its value has been significantly surpassed. In most cases the Manesty tableting press used cannot exceed a compression force of 1200 pounds (1 t = 2000 pounds) when employing PLGA as a directly compressible excipient.

Compression of the PLGA powders generates significant heat within the internal structure of the tablet. The excess heat is dissipated and escapes gradually through the surface of the tablet matrix. Since it would have required significant modification of the current testing equipment to permit data to be collected in order to monitor these in situ elevated temperatures, this phenomenon could not be explored in detail as part of the current work.

At temperatures above the T_g value, amorphous material would show a transformation in its behaviour with an increase in ductility. Subsequently what is occurring is that the material is transitioning into a more rubbery state. It is well-known that above the T_g value molecular motions are very rapid which may lead to a decrease in the extent of polymer chain entanglement and an increased mobility of the polymer chain segments, whereas below the T_g value these motions are restricted and are regarded as almost 'frozen'.

With regard to the DSMT device, the study commenced employing 1 t of uniaxial compression force, which has already exceeded the yield pressure (>1200 pounds), resulting in increased heat generation and dissipation, that is well above the

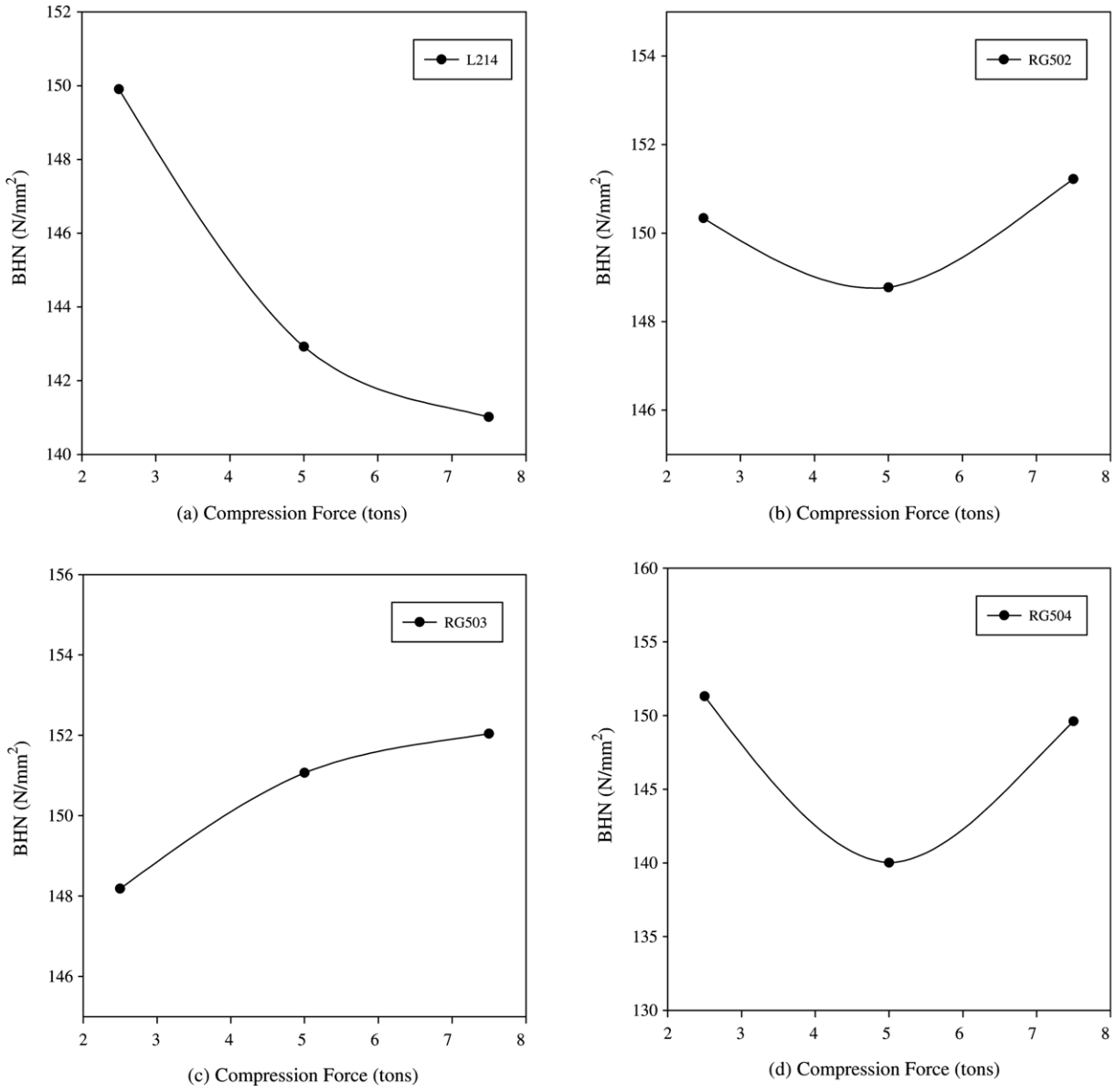

Fig. 5. (a–d) Compressibility profiles of the various polymers investigated.

stated T_g value. This excess heat induces structural changes at a molecular level and causes a deformation of the matrix that leads to stress relief at heterogeneous stress loci distributed within the tablet matrix. Consequently, stress relaxation and surface disruption occur on a micro-level.

This is consistent with the broader expectation that amorphous type materials have a higher free energy. Essentially, the greater the compression force, more heat is generated when above the yield value, which results in exceeding the T_g value. The DSMT consequently turns into a more rubbery state and therefore the higher compression force produces a 'softer' matrix.

3.2. Erodibility of the DSMT device

Table 4 lists the residual masses obtained for the DSMT devices investigated. The effect of the various polymer grades

Table 4
Residual masses and % mass loss at various time intervals

Polymer type and time	Residual masses (mg) ± S.D.	%Mass loss[a]
Resomer® RG502		
At 8 weeks	49.75 ± 5.05	48.35
At 12 weeks	46.75 ± 8.18	51.47
At 24 weeks	44.90 ± 5.98	53.39
Resomer® RG503		
At 8 weeks	55.23 ± 5.01	42.09
At 12 weeks	49.65 ± 8.41	47.94
At 24 weeks	46.25 ± 5.59	51.50
Resomer® RG504		
At 8 weeks	61.70 ± 4.10	35.53
At 12 weeks	53.60 ± 8.06	43.99
At 24 weeks	49.50 ± 6.93	48.37

[a] Calculated using Eq. (2).

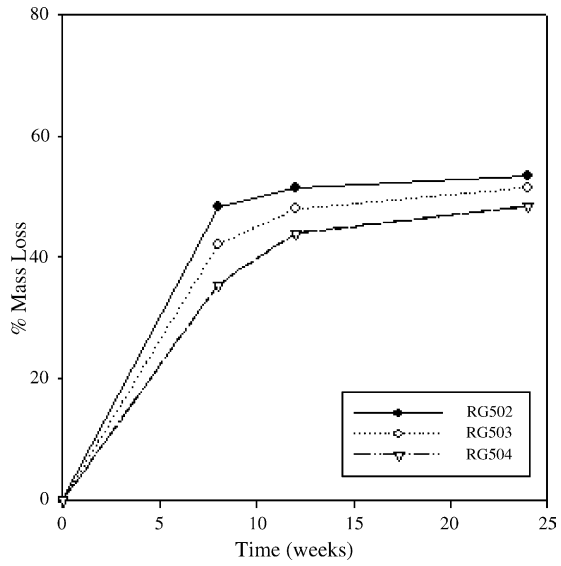

Fig. 6. Mass loss profiles of DSMT devices using various grades of PLGA as a function of erosion time.

used in fabricating the DSMTs on mass loss profiles are shown in Fig. 6. The shapes of the curves were found to be similar for all the investigated polymers. As seen from Fig. 6, the composition of the polymers employed in fabricating the DSMTs have a significant effect on the mass loss profile, or otherwise the erosion characteristics.

3.3. Scanning electron microscopy

The morphological characteristics of the DSMT devices undergoing erosion at various predetermined time intervals are shown in Figs. 7 and 8. The photomicrographs were taken of a sample used for determining gravimetric changes as described earlier.

Before storage in SVH at 37 °C, the surface of the DSMT device appeared smooth without many cracks and pores visible within the matrix (Figs. 7a and 8a). After 8 weeks of storage (Figs. 7b and 8b) the DSMT surface was still fairly smooth, but a few superficial cracks emerged. These cracks were probably due to the drying process during SEM sample preparation. Furthermore, it did not show any channel-like structures, not allowing much diffusion of dissolution medium into the device matrix. At 12 weeks, (Fig. 7c) surface pores and cracks were prominently engulfing the matrix, resulting in channel-like structures that permit easy diffusion of release medium into the drug delivery system. At this stage the DSMT device began to evidently show signs of size reduction.

This can be noticeably seen in Fig. 7d by the outstanding porous surface with a vast amount of cracks and channel-like structures appearing after 24 weeks of incubation. During observation, the cracks vaguely increased, indicating a looser structure of the matrix as the device continued to erode.

3.4. In vitro release studies

In general, the release profiles of both antiviral bioactives from the biodegradable polymer matrices have a biphasic release pattern: an initial burst and a second phase that is derived from diffusional release before the onset of polymer erosion. The initial burst may have resulted from the rapid release of the drugs deposited on the surface of the matrix. During the diffusion phase, the bioactives were released slowly, and possibly was

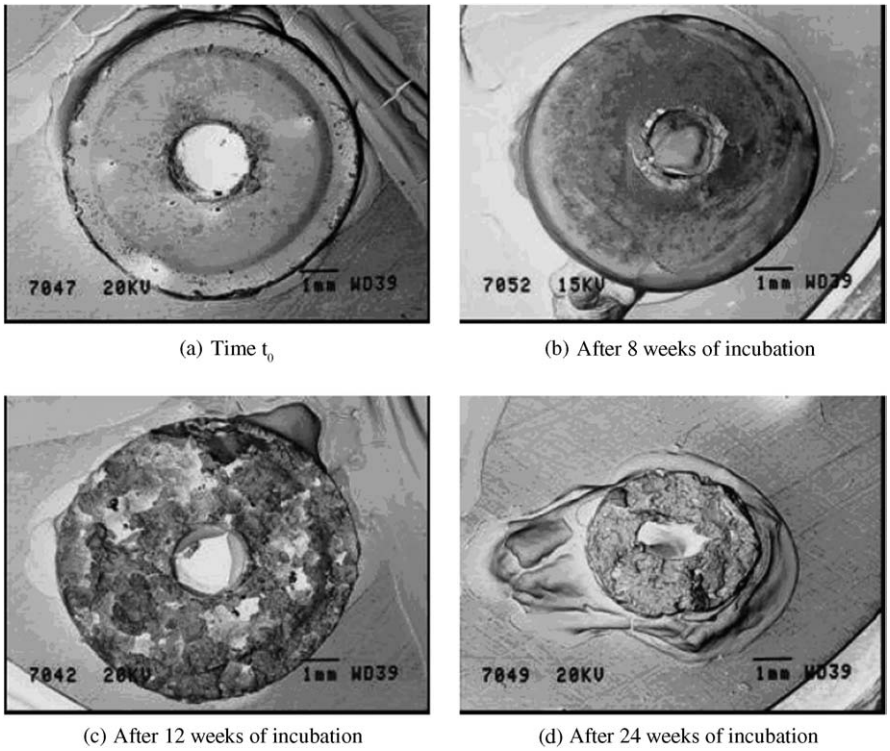

(a) Time t_0 (b) After 8 weeks of incubation

(c) After 12 weeks of incubation (d) After 24 weeks of incubation

Fig. 7. Typical scanning electron microscope images of DSMT eroding in SVH over a 24 week period.

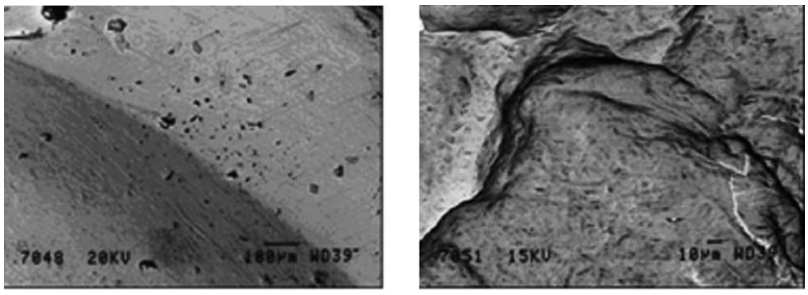

Fig. 8. Typical scanning electron microscope images of the surface of a DSMT eroding in SVH over an 8 week period.

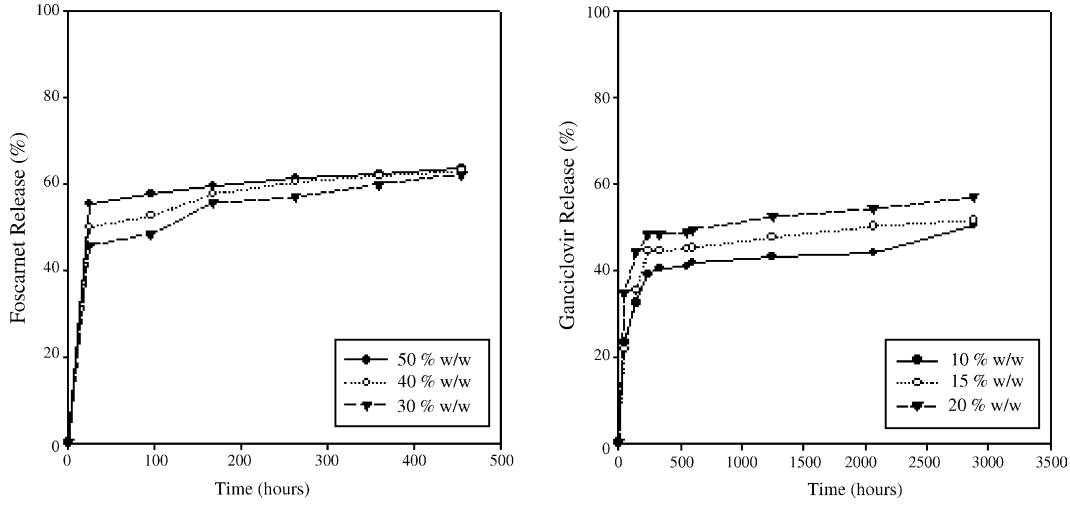

Fig. 9. Effect of foscarnet and ganciclovir loading on the in vitro release from the Resomer® RG504 DSMT device.

controlled by the degradation rate of the polymer and the drug loading. The rate of release in the diffusion phase tended to be more prolonged in the DSMT's consisting of the polymer with the higher inherent viscosities. An increase in the drug load of the device may also increase the release rate and an overload of drug may result in the release of a large amount of drug as an initial burst.

The release kinetics during the second phase was fairly consistent at the various drug-loading concentrations. The devices have a biphasic pattern and in the higher viscosity polymer, the duration of drug release tends to be more prolonged (Figs. 9 and 10). Ideally, an in vivo release rate of 0.04 μg/h will be targeted based on the Vitrasert® implant.

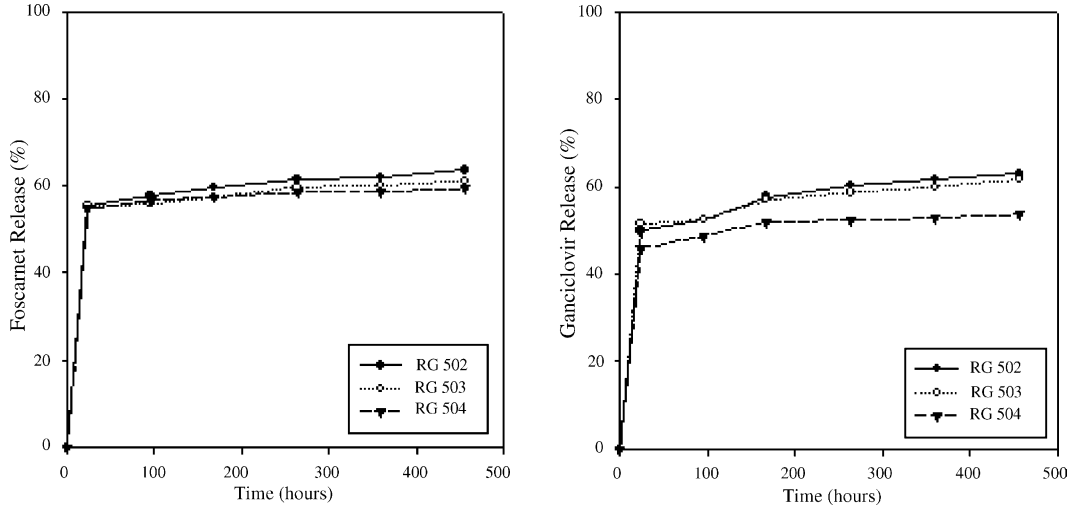

Fig. 10. The effect of PLGA viscosity on the in vitro release from the DSMT device at a constant bioactive load.

4. Conclusion

PLGA can be regarded as suitably compressible for designing implantable devices such as the DSMT using relatively low compression forces which aid in trouble-free manufacturing with regard to wear on major tableting equipment such as punches and dies. The veracity of the compact structure of the DSMT device was retained even after 24 weeks of incubation during the erosion studies, indicating that the device is suitable as a biodegradable drug delivery system.

The DSMT device generally has a biphasic release pattern: an initial burst and a diffusional phase. The inherent viscosity of the polymers employed and the drug loading characteristics affects the duration and rate of bioactive release. These factors are able to regulate the release profile from the DSMT device in order to achieve the desired release kinetics of the drug delivery system. The DSMT with a superior load of bioactive had a larger quantity of bioactive released during the initial phase.

The DSMT has proved to be a flexible and versatile biodegradable intraocular drug delivery system that provides rate-modulated release of antiviral bioactives to the posterior segment of the eye and may be suitable for the treatment of CMV-R.

Acknowledgements

The Medical Research Council (MRC) and the National Research Foundation (NRF) of South Africa are acknowledged for the grants awarded.

References

Ashton, P., Brown, J.D., Pearson, P.A., 1992. Intravitreal ganciclovir pharmacokinetics in rabbits and man. J. Ocular. Pharmacol. 8, 343–347.

Cochereau-Massin, I., Lehoang, P., Lautier-Frau, M., Zazoun, L., Marcel, P., Robinet, M., Matheron, J., Katlanici, C., Gharakhanian, S., Rosenbaum, W., Ingrand, D., Gentilini, M., 1991. Efficacy and tolerance of intravitreal ganciclovir in cytomegalovirus retinitis in acquired immune deficiency syndrome. Ophthalmology 98, 1348–1355.

Davis, J.L., Tabandeh, H., Feuer, W.J., Kumbhat, S., Roth, D.B., Chaudry, N.A., 1999. Effect of potent antiretroviral therapy on recurrent cytomegalovirus retinitis treated with the ganciclovir implant. Am. J. Ophthalmol. 127, 283–287.

Diaz-Llopis, M., Espana, E., Munoz, et al., 1994. High dose intravitreal foscarnet in the treatment of cytomegalovirus retinitis in AIDS. Br. J. Ophthalmol. 78, 120–124.

Hatton, M.P., Duker, J.S., Reichel, E., Morley, M.G., Puliafito, A., 1998. Treatment of relapsed cytomegalovirus retinitis with the sustained-release ganciclovir implant. Retina 18, 50–55.

Herroro-Vanrell, R., Ramirez, L., 2000. Biodegradable PLGA microspheres loaded with ganciclovir for intraocular administration. Encapsulation technique, in vitro release profiles, and sterilization process. Pharm. Res. 17, 1323–1328.

Holbrook, J.T., Jabs, D.A., Weinberg, D.V., Lewis, R.A., Davis, M.D., Freidberg, D., 2003. Visual loss in patients with cytomegalovirus retinitis and acquired immunodefiency syndrome before widespread availability of highly active antiretroviral therapy. Arch. Ophthalmol. 121, 99–107.

Holland, G.N., Sidikaro, Y., Krieger, A.E., Hardy, D., Sakamoto, M., Frenkel, L., Winston, D., Gottlieb, M., Bryson, Y., Champlin, R., Ho, W., Winters, R., Wolfe, P., Cherry, J., 1987. Treatment of cytomegalovirus retinopathy with ganciclovir. Ophthalmology 94, 815–822.

Holland, G.N., Buhles, W.C., Mastre, B., Kaplan, H.J., 1989. A controlled retrospective study of ganciclovir treatment for cytomegalovirus retinopathy: use of standardized system for the assessment of disease outcome, for the ULCA CMV retinopathy study group. Arch. Ophthalmol. 107, 1759–1766.

Jabs, D.A., Martin, B., Forman, M.S., Hubbard, L., Dunn, J.P., Kempen, J.H., Davis, J.L., Weinberg, D.V., 2003. The cytomegalovirus retinitis and viral resistance study group, Cytomegalovirus resistance to ganciclovir and clinical outcomes of patients with cytomegalovirus retinitis. Am. J. Ophthalmol. 135, 26–34.

Kumar, M.T., Pandit, J.K., Balasubramaniam, J., 2001. Novel therapeutic approaches for uveitis and retinitis. J. Pharm. Pharmaceut. Sci. 4, 248–254.

Lin, D.Y., Warren, J.F., Lazzeroni, L.C., Wolitz, R.A., Mansour, S.E., 2002. Cytomegalovirus retinitis after initiation of highly active antiretroviral therapy in HIV-infected patients. Retina 22, 268–277.

Martin, D.F., Ferris, F.L., Parks, D.J., Walton, R.C., Mellow, S.D., Gibbs, D., Remaley, N.A., Ashton, P., Davis, M.D., Chan, C., Nussenblatt, R.B., 1997. Ganciclovir implant exchange. Timing, surgical procedure, and complications. Arch. Ophthalmol. 115, 1389–1394.

Merodio, M., Arnedo, A., Renedo, M.J., Irache, J.M., 2001. Ganciclovir-loaded albumin nanoparticles: preparation and characterization of their in vitro release properties. Eur. J. Pharm. Sci. 12, 251–259.

Musch, D.C., Martin, D.F., Matthew, D., Davis, M.D., Kupperman, B.D., Gordon, J.F., 1997. Treatment of cytomegalovirus retinitis with a sustained-release ganciclovir implant. N. Engl. J. Med. 337, 83–90.

Perkins, S.L., Yang, C., Ashton, P., Jaffe, G.J., 2001. Pharmacokinetics of the ganciclovir implant in the silicone-filled eye. Retina 21, 10–14.

Rosanne, M.O., 2001. Technology evaluation: Formivirsen, Isis Pharmaceuticals, Inc./CIBA Vision. Curr. Opin. Mol. Ther. 3, 288–294.

Sanborn, G.E., Anand, R., Torti, R.E., Nightingale, S.D., Cal, S.X., Yates, B., Ashton, P., Smith, T., 1992. Sustained-release ganciclovir therapy for treatment of cytomegalovirus retinitis. Arch. Ophthalmol. 110, 188–195.

Smith, T.J., Pearson, P.A., Blanford, D.L., Brown, J.D., Goins, K.A., 1992. Intravitreal sustained-release ganciclovir. Arch. Ophthalmol. 110, 255–258.

Yasukawa, T., Kimura, H., Kunou, N., Miyamoto, H., Honda, Y., Ogura, Y., Ikada, Y., 2000. Biodegradable scleral implant for intravitreal controlled release of ganciclovir. Graefe's Arch. Clin. Exp. Ophthalmol. 238, 186–190.

Zhang, X., Wyss, U.P., Pichora, D., Goosen, M.F.A., 1992. An investigation of poly(lactic acid) degradation. J. Bioact. Compat. Polym. 9, 80–100.